Organometallics **1994,** *13,* 4237−4245

Theoretical Studies of Organometallic Compounds. 9. Structures and Bond Energies of the Methylcuprates CH_3Cu, $(CH_3)_2Cu^-$, $(CH_3)_2CuLi$, $(CH_3)_2CuLi{\cdot}H_2O$, $[(CH_3)_2CuLi]_2$, and $[(CH_3)_2CuLi]_2{\cdot}2H_2O$[1]

Marlis Böhme,[†] Gernot Frenking,[*,†] and Manfred T. Reetz[‡]

Fachbereich Chemie, Philipps-Universität Marburg, Hans-Meerweinstrasse,
D-35032 Marburg, Germany, and Max-Planck-Institut für Kohlenforschung,
Kaiser-Wilhelm-Platz 1, D-45470 Mülheim/Ruhr, Germany

Received February 23, 1994[⊗]

The geometries of the copper compounds CH_3Cu (**1**), $(CH_3)_2Cu^-$ (**2**), $(CH_3)_2CuLi$ (**3**), $(CH_3)_2CuLi{\cdot}H_2O$ (**4**), $[(CH_3)_2CuLi]_2$ (**5**), and $[(CH_3)_2CuLi]_2{\cdot}2H_2O$ (**6**) are optimized at the HF and MP2 level of theory, using an effective core potential for Cu and all-electron basis sets for the other atoms. The Cu−C bond strength is calculated at correlated levels, and the electronic structure of **1**−**6** is investigated using the topological analysis of the electron density distribution and the natural bond orbital partitioning scheme. The optimized geometries at the MP2 level appear to be reliable, while the HF optimized structures have Cu−C bond lengths which are too long. Methylcopper (**1**) is predicted with a Cu−C bond length of 1.923 Å and a Cu−C bond strength D_o = 45. 0 kcal/mol. Dimethylcuprate anion (**2**) has a linear (D_{3h}) structure and slightly longer Cu−C bond distances (1.963 Å) than **1**. The global energy minimum structure of the monomeric form of Gilman's reagent $(CH_3)_2CuLi$ (**3d**) is predicted with an open (noncyclic) geometry and a nearly linear CH_3−Cu−CH_3 moiety. The lithium atom in **3d** is coordinated to only one methyl group. The cyclic forms with a bridging lithium atom are no energy minima on the potential energy hypersurface at the MP2 level of theory. Complexation of **3** by one water molecule at Li does not influence the geometries and relative energies of the open and cyclic forms. The global energy minimum structure of $(CH_3)_2CuLi{\cdot}H_2O$ (**4**) is **4d**, which has an open (noncyclic) geometry with a nearly linear CH_3−Cu−CH_3 moiety. The dimeric form of Gilman's reagent $[(CH_3)_2CuLi]_2$ (**5**) has a planar cyclic geometry with D_{2h} symmetry. Complexation of **5** at the lithium atoms by two water molecules gives $[(CH_3)_2CuLi]_2{\cdot}2H_2O$ (**6**). The geometry optimization of **6** yields two energetically nearly degenerate forms **6a,b** with slightly twisted geometries which deviate only little from D_{2h} symmetry. The analysis of the electronic structure shows that the Cu−C bonds in **1**−**6** are strongly polarized toward the carbon atom. The polar Cu−C bonds have distinct covalent contributions, however. The copper bonding has mainly s-character (~90%) as revealed by the NBO analysis.

Introduction

The preparation of the first organocuprate Me_2CuLi, which is commonly referred to as "Gilman's reagent", was reported in 1952.[2] Since then, organocopper compounds have become versatile agents in organic synthesis.[3] But in contrast to the accumulated knowledge concerning the synthetic utility of organocuprates, there is very little information about the structure of organocopper compounds. Only a few X-ray structure analyses of organocuprates are reported in the literature.[4] The experimental determination of the structures of cuprates is difficult, because the aggregation state is frequently not known and because several aggregation states may coexist in solution. The ongoing controversy about "higher order" and "lower order" cuprates[5,6] demonstrates the need for more detailed information about the structure of cuprates. The conflicting interpretation of the NMR spectra of the investigated compounds indicates the difficulties of experimental techniques to determine unambiguously the geometry of organocopper compounds.[5,6]

In principle, quantum mechanical calculations may provide additional information about the equilibrium structures, which in combination with the experimental data might help in the characterization of the structure of cuprates. However, accurate theoretical studies of transition metal compounds are believed not to be possible because of the large number of electrons at the metal. In a systematic investigation[7] of the reliability of effective core potentials (ECP) we are able to show

---

[†] Phillips-Universität Marburg.

[‡] Max-Planck-Institut für Kohlenforschung.

[⊗] Abstract published in *Advance ACS Abstracts,* October 1, 1994.

(1) Part 8: Veldkamp, A.; Frenking, G. *J. Am. Chem. Soc.* **1994,** *116,* 4937.

(2) Gilman, H.; Jones, R. G.; Woods, L. A. *J. Org. Chem.* **1952,** *17,* 1630.

(3) (a) Posner, G. H. *An Introduction to Synthesis Using Organocopper Reagents*; Wiley: New York, 1980. (b) Rossiter, B. E.; Swingle, N. M. *Chem. Rev.* **1992,** *92,* 771.

(4) Power, P. P. In *Progress in Inorganic Chemistry*; Lippard, S. J., Ed.; Wiley: New York, 1991; Vol. 39.

(5) Bertz, S. H. *J. Am. Chem. Soc.* **1990,** *112,* 4031.

(6) Lipshutz, B. H.; Sharma, S.; Ellsworth, E. L. *J. Am. Chem. Soc.* **1990,** *112,* 4032.

(7) Jonas, V.; Frenking, G.; Reetz, M. T. *J. Comput. Chem.* **1992,** *13,* 919.

0276-7333/94/2313-4237$04.50/0

that the geometries and energies of transition metal compounds can be predicted in good agreement with experiment. From this work[7] and further studies of the structures of transition metal complexes[1,8] we can expect good accuracy for the calculated geometries of Cu(I) compounds at the MP2 level (Möller–Plesset perturbation theory terminated at second order)[9] using split-valence basis sets with polarization functions in combination with an ECP for Cu.

In the present study we report the calculated geometries, bond energies, and electronic structures of the methyl cuprates CH_3Cu (**1**), $(CH_3)_2Cu^-$ (**2**), $(CH_3)_2CuLi$ (**3**), $(CH_3)_2CuLi{\cdot}H_2O$ (**4**), $[(CH_3)_2CuLi]_2$ (**5**), and $[(CH_3)_2CuLi]_2{\cdot}2H_2O$ (**6**). The electronic structure of **1**–**6** is analyzed using the topological analysis of the electron density distribution developed by Bader and co-workers[10] and the natural bond orbital (NBO) analysis developed by Weinhold and co-workers.[11]

Only very few theoretical studies of methylcuprates have been published previously. Methylcopper (**1**) was calculated by two groups,[12,13] at the Hartree–Fock (HF) level of theory. The reaction course of the addition of **1** to α,β-unsaturated carbonyl compounds has theoretically been investigated by Morokuma et al.[13] The most accurate theoretical study of **1** was published by Bauschlicher et al.,[14] who used the modified coupled pair functional approach (MCPF). Methylcopper (**1**) has also been calculated using density functional theory (DFT).[15] The optimized geometry of **2** is reported in one theoretical study of the HF level only.[16] A partially optimized geometry for the dimeric form of Gilman's reagent $[(CH_3)_2CuLi]_2$ (**5**) at the HF/STO-3G level using fixed bond distances was reported by Stewart et al.[17] There are no other theoretical studies of the equilibrium geometries of **3**–**6** known to us. We point out that isomeric structures of $(CH_3)_3CuLi_2{\cdot}2H_2O$ have theretically been investigated at the PRDDO and MP2/ECP level of theory by Snyder et al.[18]

Theoretical Details

The geometry optimizations were performed at the Hartree–Fock (HF) and MP2 level[9] of theory, using an effective core potential (ECP) for Cu developed by Hay and Wadt[19] which replaces the 1s–2p core electrons. For the 3s and 3p outer core electrons and the 4s and 3d valence electrons (19 electrons) basis functions with the contraction schemes [441/41/41] and [441/2111/41] are employed.[7] For the other atoms the all-electron basis sets 3-21G[20] and 6-31G(d)[21] were used. A set of five primitives is used for the d polarization functions. The vibrational frequencies and zero-point energies (ZPE) were calculated at the HF and MP2 levels of theory. Improved total energies were calculated using Möller–Plesset perturbation theory terminated at fourth order MP4 (SDTQ).[22] In a few cases, additional energy calculations were carried out at the MP2 and CCSD(T) level (coupled-cluster theory with single, double, and noniterative estimate of triple excitations)[23] using a larger basis set. For these calculations, the basis set for Cu was augmented by an additional set of f-type polarization functions [441/2111/41/1] with an exponent[24] of 3.525. A 6-31+G(d) basis set[21,25] was used for the other atoms. The different basis sets BS I, II, and III used in this study are summarized in Table 1.

Table 1. Notation of the Basis Sets I–III

	BS I	BS II	BS III
Cu	(ECP) [441/41/41]	(ECP) [441/2111/41]	(ECP) [441/2111/41/1]
C, H, Li, O	3-21G	6-31G(d)	6-31+G(d)

The calculations were carried out using Gaussian 90,[26] Gaussian 92,[27] TURBOMOLE,[28] and ACES II.[29] For the calculation of the electron density distribution $\varrho(\mathbf{r})$, the gradient vector field $\nabla\varrho(\mathbf{r})$, and its associated Laplacian $\nabla^2\varrho(\mathbf{r})$ the program PROAIM, SADDLE, GRID, and GRDVEC were used.[10] The NBO analysis[11] was carried out using Gaussian 92.[27]

Results and Discussion

Figure 1 shows the optimized structures of CH_3Cu (**1**), $(CH_3)_2Cu^-$ (**2**), $(CH_3)_2CuLi$ (**3**), $(CH_3)_2CuLi{\cdot}H_2O$ (**4**), $[(CH_3)_2CuLi]_2$, (**5**), and $[(CH_3)_2CuLi]_2{\cdot}2H_2O$ (**6**). Table

---

(8) (a) Jonas, V.; Frenking, G.; Reetz, M. T. *Organometallics* **1993**, *12*, 2111. (b) Stegmann, R.; Neuhaus, A.; Frenking, G. *J. Am. Chem. Soc.* **1993**, *115*, 11930. (c) Veldkamp, A.; Frenking, G. *Organometallics* **1993**, *12*, 4613. (d) Ehlers, A. W.; Frenking, G. *J. Chem. Soc., Chem. Commun.* **1993**, 1709. (e) Ehlers, A. W.; Frenking, G. *J. Am. Chem. Soc.* **1994**, *116*, 1514. (f) Ehlers, A. W.; Frenking, G. *J. Am. Chem. Soc.*, submitted for publication. (g) Neuhaus, A.; Veldkamp, A.; Frenking, G. *Inorg. Chem.*, in press.

(9) (a) Møller, C.; Plesset, M. S. *Phys. Rev.* **1934**, *46*, 618. (b) Binkley, J. S.; Pople, J. A. *Int. J. Quantum Chem.* **1975**, *9S*, 229.

(10) Biegler-König, F. W.; Bader, R. W. F.; Ting-Hua, T. *J. Comput. Chem.* **1982**, *3*, 317.

(11) (a) Reed, A. E.; Curtiss, L. A.; Weinhold, F. *Chem. Rev.* **1988**, *88*, 899. (b) Weinhold, F.; Carpenter, J. E. In *The Structure of Small Molecules and Ions*; Naaman, R., Vager, Z., Eds.; Plenum: New York, 1988; p 227.

(12) Poirier, R. A.; Ozin, J. A.; McIntosh, F.; Csizmadia, G.; Daudel, R. *Chem. Phys. Lett.* **1983**, *101*, 221.

(13) (a) Dorigo, A. E.; Morokuma, K. J. *J. Chem. Soc., Chem. Commun.* **1989**, 1884. (b) Dorigo, A. E.; Morokuma, K. J. *J. Am. Chem. Soc.* **1989**, *111*, 4635. (c) Nakamura, E.; Nakamura, M.; Miyachi, Y.; Koga, N.; Morokuma, K. *J. Am. Chem. Soc.* **1993**, *115*, 99.

(14) Bauschlicher, C. W.; Langhoff, S. R.; Partidge, H.; Barnes, L. A. *J. Chem. Phys.* **1989**, *91*, 2399.

(15) Ziegler, T.; Tschinke, V.; Becke, A. *J. Am. Chem. Soc.* **1987**, *109*, 1351.

(16) Dobbs, K. D.; Hehre, W. J. *J. Comput. Chem.* **1987**, *8*, 861.

(17) Stewart, K. R.; Lever, J. R.; Wangbo, M.-H. *J. Org. Chem.* **1982**, *47*, 1472.

(18) (a) Snyder, J. P.; Tipsworth, G. E.; Spangler, D. P. *J. Am. Chem. Soc.* **1992**, *114*, 1507. (b) Snyder, J. P.; Spangler, D. P.; Behling, J. R. *J. Org. Chem.* **1994**, *59*, 2665.

(19) Hay, P. J.; Wadt, W. R. *J. Chem. Phys.* **1985**, *82*, 299.

(20) Hehre, W. J.; Ditchfield, R.; Pople, J. A. *J. Chem. Phys.* **1972**, *56*, 2257.

(21) (a) Hehre, W. J.; Ditchfield, R.; Pople, J. A. *J. Chem. Phys.* **1972**, *76*, 163. (b) Frisch, M. J.; Pople, J. A.; Binkley, J. S. *J. Chem. Phys.* **1984**, *80*, 3265.

(22) (a) Krishnan, R.; Pople, J. A. *Int. J. Quantum. Chem.* **1978**, *14*, 91. (b) Krishnan, R.; Frisch, M. J.; Pople, J. A. *J. Chem. Phys.* **1980**, *72*, 4244.

(23) (a) Cizek, J. *J. Chem. Phys.* **1966**, *45*, 4256. (b) Pople, J. A.; Krishnan, R.; Schlegel, H. B.; Binkley, J. S. *Int. J. Quantum Chem.* **1978**, *14*, 545. (c) Bartlett, R. J.; Purvis, G. D. *Ibid.* **1978**, *14*, 561. (d) Purvis, G. D.; Bartlett, R. J. *J. Chem. Phys.* **1982**, *76*, 1910. (e) Raghavachari, K.; Trucks, G. W.; Pople, J. A.; Head-Gordon, M. *Chem. Phys. Lett.* **1989**, *157*, 479. (f) Bartlett, R. J.; Watts, J. D.; Kucharski, S. A.; Noga, J. *Ibid.* **1990**, *165*, 513.

(24) Ehlers, A. W.; Böhme, M.; Dapprich, S.; Gobbi, A.; Höllwarth, A.; Jonas, V.; Köhler, K. F.; Stegmann, R.; Veldtkamp, A.; Frenking, G. *Chem. Phys. Lett.* **1993**, *208*, 111.

(25) Clark, T.; Chandrasekhar, J.; Spitznagel, G. W.; Schleyer, P. v. R. *J. Comput. Chem.* **1983**, *4*, 294.

(26) *Gaussian 90, Revision F.* Frisch, M. J.; Head-Gordon, M.; Trucks, G. W.; Foresman, J. B.; Schlegel, H. B.; Raghavachari, K.; Robb, M. A.; Binkley, J. S.; Gonzales, C.; Defrees, D. J.; Fox, D. J.; Whiteside, R. A.; Seeger, R.; Melius, C. F.; Baker, J.; Martin, R. L.; Kahn, L. R.; Stewart, J. J. P.; Topiol, S.; Pople, J. A. Gaussian, Inc.: Pittsburgh, PA, 1990.

(27) *Gaussian 92, Revision C.* Frisch, M. J.; Trucks, G. W.; Head-Gordon, M.; Gill, P. M. W.; Wong, M. W.; Foresman, J. B.; Johnson, B. G.; Schlegel, H. B.; Robb, M. A.; Replogle, E. S.; Gomperts, R.; Andres, J. L.; Raghavachari, K.; Binkley, J. S.; Gonzales, C.; Martin, R. L.; Fox, D. J.; Defrees, D. J.; Baker, J.; Stewart, J. J. P.; Pople, J. A. Gaussian, Inc.: Pittsburgh, PA, 1992.

(28) (a) Häser, M.; Alrichs, R. *J. Comput. Chem.* **1989**, *10*, 104. (b) Alrichs, R.; Bär, M.; Häser, M.; Horn, H.; Kölmel, C. *Chem. Phys. Lett.* **1989**, *162*, 165. (c) Horn, H.; Weiss, H.; Häser, M.; Ehrig, M.; Alrichs, R. *J. Comput. Chem.* **1991**, *12*, 1058. (d) Häser, M.; Almlöf, J.; Feyereisen, M. W. *Theor. Chim. Acta* **1991**, *79*, 115.

(29) ACES II, an ab initio program system written by: Stanton, J. F.; Gauss, J.; Watts, J. D.; Lauderdale, W. J.; Bartlett, R. J. University of Florida, Gainsville, FL, 1991.

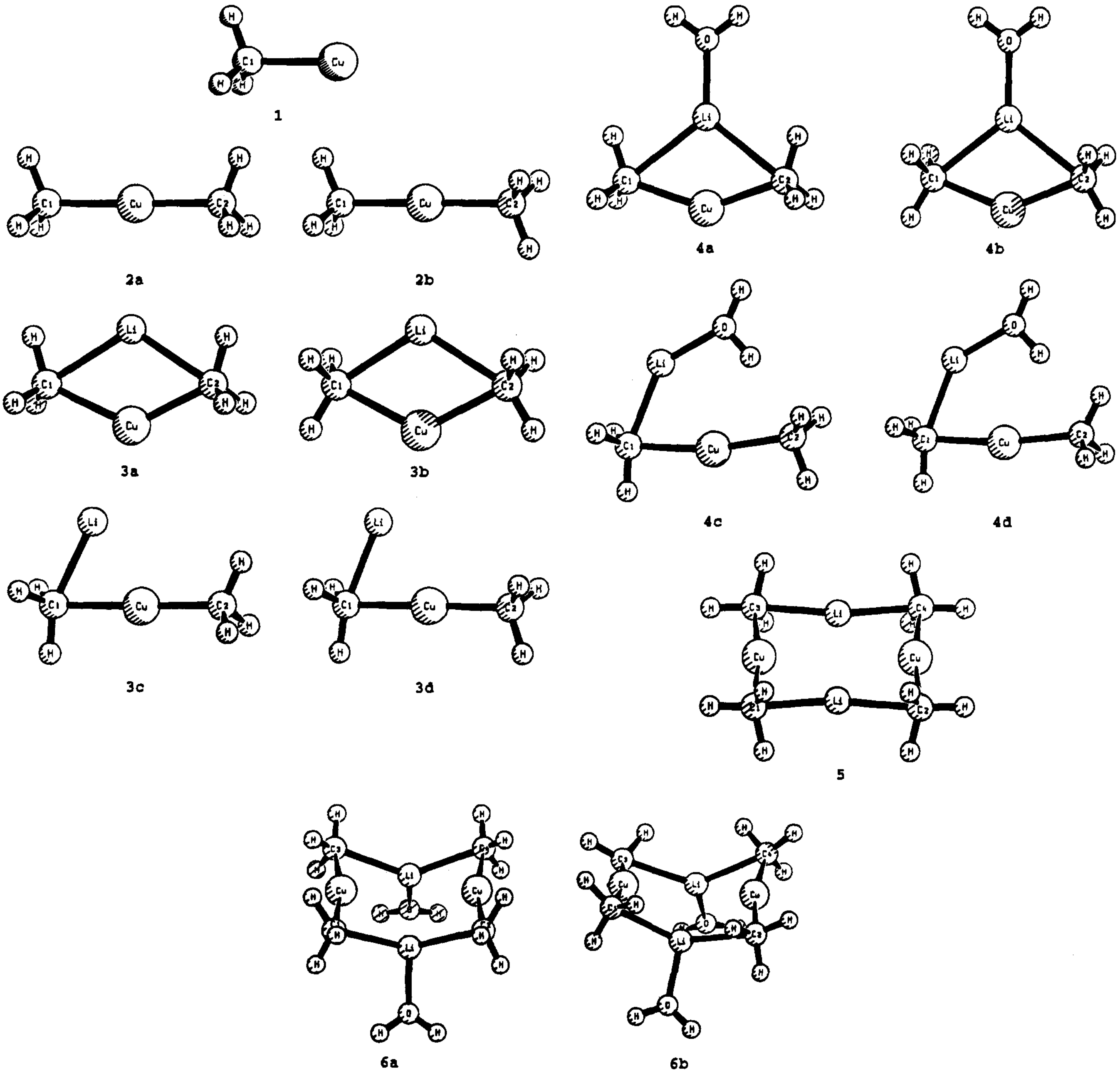

Figure 1. Optimized structures of CH_3Cu (**1**), $(CH_3)_2Cu^-$ (**2a,b**), $(CH_3)_2CuLi$ (**3a–d**), $(CH_3)_2CuLi{\cdot}H_2O$ (**4a–d**), $[(CH_3)_2CuLi]_2$ (**5**), and $[(CH_3)_2CuLi]_2{\cdot}2H_2O$ (**6a,b**).

2 lists the optimized geometry parameters. Table 3 gives the calculated total energies and zero-point energies for the compounds **1**–**6**.

The optimized structure of methylcopper (**1**) has C_{3v} symmetry. It is interesting that the Cu–C bond length of **1** calculated at the HF level is the same (2.005 Å) using basis sets I and II (Table 1). The calculated Cu–C bond distance of 2.005 Å is similar to the values at the HF level of theory reported by other workers (1.991,[12] 2.040 Å [13b]). The higher value of 2.040 Å reported by Dorigo and Morokuma[13b] is probably due to the large-core ECP (11 valence electrons) used by these authors. At the MP2/II level, the Cu–C distance is predicted to be 1.923 Å, which is significantly shorter than the HF value. Previous studies have shown[8c–e] that metal–ligand distances of transition metal complexes in *low* oxidation states calculated at the MP2 level are in good agreement with experimental values, while the bond lengths predicted at the HF level are too long. The optimized geometries of cuprates reported here are in agreement with this observation.[8c–e] The MP2/II value of 1.923 Å for the Cu–C bond length of **1** is close to the MCPF result of 1.936 Å.[14] The reported bond length of 1.86 Å using DFT techniques is probably too short.[15] The good agreement of the HF value (2.005 Å) with the measured Cu–C bond length of 2.04 ± 0.05 Å for the crystal structure of an alkylcopper tetramer[30] is probably fortuitous. The copper atoms in the tetramer are dicoordinated. Our results for **2**–**6** indicate that dicoordinated Cu complexes have longer Cu–C distances than monocoordinated complexes.[31]

We calculated the Cu–CH_3 bond strength of **1**. Table 4 presents the theoretically predicted dissociation ener-

---

[30] Jarvis, J. A.; Killbourn, B. T.; Pearce, R.; Lappert, M. F. *J. Chem. Soc., Chemm. Commun.* **1973**, 475.

[31] The only available experimental value for a monocoordinated Cu–C compound has been published for a Cu–phenyl complex. The Cu–C distance of Cu–C_6H_5 calculated at MP2/II is 1.900 Å (Böhme, M.; Frenking, G. To be published. The experimental value is 1.890 Å: Lingnau, R.; Strähle, J. *Angew. Chem.* **1988**, *100*, 409; *Angew. Chem., Int. Ed. Engl.* **1988**, *27*, 436.

Table 2. Optimized Bond Distances r_{A-B} (Å), Angles (deg), and Torsion Angles (deg) of the Calculated Structures 1−6

no.	sym	r_{C^1-Cu}	r_{Cu-C^2}	r_{C^1-Li}	r_{Li-C^2}	α_{C-Cu-C}	r_{Cu-Cu}	τ^a	method
1	C_{3v}	2.005							HF/I
		2.005							HF/II
		1.923							MP2/II
2a	D_{3h}	2.025	2.025			180.0			HF/I
		2.053	2.053			180.0			HF/II
		1.963	1.963			180.0			MP2/II
2b	D_{3d}	2.025	2.025			180.0			HF/I
		2.054	2.054			180.0			HF/II
		1.963	1.963			180.0			MP2/II
3a	C_{2v}	2.113	2.113	2.277	2.277	129.3			HF/I
		2.147	2.147	2.272	2.272	126.9			HF/II
		1.971	1.971	2.574	2.574	155.4			MP2/II
3b	C_{2v}	2.127	2.127	2.236	2.236	126.2			HF/I
		2.164	2.164	2.233	2.233	123.2			HF/II
		1.965	1.965	2.650	2.650	161.0			MP2/II
3c	C_1	2.010	1.915	2.058	3.687	179.8			MP2/II
3d	C_1	2.009	1.916	2.058	3.692	179.9			MP2/II
4a	C_{2v}	2.058	2.058	2.470	2.470	143.3			HF/I
		2.106	2.106	2.412	2.412	136.4			HF/II
		1.959	1.959	2.658	2.658	160.8			MP2/II
4b	C_{2v}	2.076	2.076	2.400	2.400	137.9			HF/I
4c	C_1	2.086	2.023	2.121	3.742	169.8			HF/I
		2.118	2.033	2.097	3.763	168.5			HF/II
4d	C_1	1.998	1.942	2.077	3.731	175.2			MP2/II
5	D_{2h}	2.057	2.057	2.086	2.086	172.7	3.878	180.0	HF/I
		2.066	2.066	2.069	2.069	174.2	3.904	180.0	HF/II
		1.968	1.968	2.043	2.043	174.2	3.826	180.0	MP2/II
6a	C_{2v}	2.047	2.047	2.211	2.211	169.1	3.753	173.1	HF/I
		2.062	2.062	2.194	2.194	169.1	3.758	174.2	HF/II
		1.982	1.982	2.255	2.255	167.7	3.763	177.0	MP2/I
6b	C_2	2.047	2.047	2.214	2.205	169.3	3.731	165.9	HF/I
		2.064	2.063	2.203	2.189	173.0	3.588	147.1	HF/II
		1.983	1.983	2.259	2.240	168.5	3.775	177.5	MP2/I

[a] Torsion angle $\tau(C^2-Cu-C^4-Li)$.

gies at the MP2, MP3, and MP4 levels of theory using basis set II and at the MP2 and CCSD(T) level using basis set III. Previous theoretical studies using the MCPF approach give a "best" value for D_o = 49.9 kcal/mol after estimated corrections are made for relativistic effects and basis set incompletion.[14] The directly calculated MCPF value is D_o = 45.8 kcal/mol.[14] The theoretical value using DFT techniques is D_e = 56.9 kcal/mol.[15] Experimentally, the Cu−CH_3 bond strength is estimated as 55 ± 4 kcal/mol.[32] Our theoretical values (Table 4, reaction I) are in good agreement with the theoretical and experimental estimates. The Cu−CH_3 bond strength is predicted to be 47.0, 36.5, and 53.3 kcal/mol at MP2/II, MP3/II, and MP4/II, respectively (Table 4, reaction I). An oscillating behavior of the calculated energies using Möller−Plesset perturbation theory for transition metal complexes has been found earlier.[1,33] The CCSD(T) value D_o = 45.0 kcal/mol is in excellent agreement with the previous theoretical value 45.8 kcal/mol predicted at the MCPF level.[14] We think that the bond energies calculated at CCSD(T) should be reliable.[34]

The dimethylcuprate anion (**2**) is the only methylcuprate whose geometry is known from X-ray diffraction analysis.[35] The $(CH_3)_2Cu^-$ anion in $[Li(12\text{-crown-}4)_2][(CH_3)_2Cu]$ has a linear structure with a Cu−C distance of 1.935 Å and staggered methyl groups. The calculated Cu−C bond lengths of **2a,b** at HF/I (2.025 Å) and at HF/II (2.054 Å) are longer than the experimental value. At the MP2/II level a better agreement of the theoretical Cu−C bond length (1.963 Å) with the experimental result (1.935 Å) is achieved. The calculations predict that the eclipsed conformer **2a** and the staggered form **2b** are energetically nearly degenerate (Table 3). The D_{3h} structure **2a** is a minimum at HF/II and MP2/II. The calculated bond strength $(CH_3\text{-}Cu-CH_3)^-$ of **2a** is 106.1, 93.4, and 115.8 kcal/mol at MP2/II, MP3/II, and MP4/II, respectively (Table 4, reaction II). Thus, the MP*n* series shows again oszillating bond energies. The lower D_o value at MP2/III (83.5) indicates that the addition of diffuse functions has a significant influence on the calculated bond energy of the cuprate anion. The calculated Cu−C bond strength of **2a** at CCSD(T)/III is D_o = 77.5 kcal/mol.

Several isomeric forms (**3a−d**) were calculated for the monomeric form of Gilman's reagent $(CH_3)_2CuLi$ (**3**) (Figure 1). Geometry optimization of bridged forms with C_{2v} symmetry yields the conformers **3a,b**. Structure **3a** is an energy minimum at HF/I and HF/II, while **3b** has two imaginary frequencies which belong to the rotation of the methyl groups. At MP2/II both conformations **3a,b** are not minima on the potential energy surface. Relaxation of symmetry constraints leads to the open structures **3c,d**, which have a nearly linear $(CH_3)_2Cu^-$ fragment with the Li atom coordinated to only one methyl group. The open forms **3c,d** have one Cu−C bond which is shorter and one Cu−C bond which is longer than in the cyclic forms **3a,b** (Table 2). Structure **3c** has one imaginary frequency at MP2/II, which corresponds to the rotation of the monocoordinated methyl group. The isomeric form **3d** is a

---

(32) Armentrout, P. B.; Georgiadis, R. *Polyhedron* **1988**, *7*, 1573.

(33) (a) Jonas, V.; Frenking, G.; Gauss, J. *Chem. Phys. Lett.* **1992**, *194*, 109. (b) Neuhaus, A.; Frenking, G.; Huber, C.; Gauss, J. *J. Inorg. Chem.* **1992**, *31*, 5355.

(34) Total Energies (au) of $CH_3(^2A_1)$ and $Cu(^1S)$, respectively: −39.66963, −195.26489 (MP2/II); −39.68566, −195.18234 (MP3/II); −39.69020, −195.28665 (MP4/II); −39.67330, −195.43495 (MP2/III). Total Energies (au) of $CH_3(^2A_1)$, $Cu(^1S)$, $CuCH_3$, respectively, at (CCSD(T)/III): −39.69572, −195.40323, −235.10857.

(35) Hope, H.; Olmstead, M. M.; Power, P. P.; Sandell, J.; Xu, X. *J. Am. Chem. Soc.* **1985**, *107*, 4337.

Table 3. Total Energies $E_{tot.}$ (hartrees), Relative Energies E_{rel} (kcal/mol), Number and Wavenumber (cm^{-1}) of Imaginary Frequencies *i*, and Zero-Point Energies ZPE (kcal/mol) of the Calculated Structures 1–6

no.	sym	$E_{tot.}$	E_{rel}	ZPE	*i*	level of theory
1	C_{3v}	−234.356 96		20.6	0	HF/I
		−234.574 04		20.4	0	HF/II
		−235.014 10		20.2	0	MP2/II
		−234.930 93				MP3/II[a]
		−235.066 50				MP4/II[a]
		−235.190 69				MP2/III[a]
		−235.173 49				CCSD(T)/III[a]
2a	D_{3h}	−273.744 53	0.0	39.9	1 (−4)	HF/I
		−274.180 56	0.0	39.4	0	HF/II
		−274.791 08	0.0	40.3	0	MP2/II
		−274.702 46	0.0			MP3/II[a]
		−274.880 36	0.0			MP4/II[a]
		−274.979 50	0.0			MP2/III[a]
		−274.975 45	0.0			CCSD(T)/III[a]
2b	D_{3d}	−273.744 52	<0.1	39.9	1 (−17)	HF/I
		−274.180 55	<0.1	39.4	1 (−24)	HF/II
		−274.791 05	<0.1	40.3	1 (−32)	MP2/II
		−274.702 47	<0.1			MP3/II[a]
		−274.880 25	<0.1			MP4/II[a]
		−274.979 45	<0.1			MP2/III[a]
		−274.975 41	<0.1			CCSD(T)/III[a]
3a	C_{2v}	−281.160 87	0.0	41.0	0	HF/I
		−281.641 18	0.0	40.7	0	HF/II
		−282.253 46	0.0	41.6	1 (−124)	MP2/II
		−282.166 24	0.0			MP3/II[a]
		−282.343 96	0.0			MP4/II[a]
		−282.435 72	0.0			MP2/III[a]
		−282.433 29	0.0			CCSD(T)/III[a]
3b	C_{2v}	−281.160 74	0.1	41.0	2 (−26, −14)	HF/I
		−281.640 78	0.3	40.3	2 (−71, −60)	HF/II
		−282.250 95	1.6	41.2	3 (−187, −126, −118)	MP2/II
3c	C_1	−282.258 50	−3.2	41.2	1 (−39)	MP2/II
3d	C_1	−282.258 61	−3.2	41.9	0	MP2/II
		−282.166 77	−0.3			MP3/II[a]
		−282.353 88	−6.2			MP4/II[a]
		−282.441 09	−3.4			MP2/III[a]
		−282.436 77	−2.2			CCSD(T)/III[a]
4a	C_{2v}	−356.804 60	0.0	55.2	1 (−47)	HF/I
		−357.684 74	0.0	54.9	1 (−58)	HF/II
		−358.493 03	0.0	55.3	2 (−145, −100)	MP2/II
		−358.409 43	0.0			MP3/II[a]
		−358.595 19	0.0			MP4/II[a]
		−358.683 22	0.0			MP2/III[a]
4b	C_{2v}	−356.804 38	0.1	54.9	3 (−65, −18, −14)	HF/I
4c	C_1	−356.813 87	−5.8	56.5	0	HF/I
		−357.689 51	−3.0	56.4	0	HF/II
4d	C_1	−358.502 67	−6.1	56.5	0	MP2/II
		−358.418 88	−5.9			MP3/II[a]
		−358.603 72	−5.4			MP4/II[a]
		−358.689 96	−4.2			MP2/III[a]
5	D_{2h}	−562.421 98		85.2	0	HF/I
		−563.369 76		84.2	0	HF/II
		−564.630 71		86.2	0	MP2/II
		−564.450 50				MP3/II[a]
		−564.822 40				MP4/II[a]
6a	C_{2v}	−713.686 02	0.0	114.0	0	HF/I
		−715.434 57	0.0	133.3	1 (−21)	HF/II
		−714.781 06	0.0			MP2/I
		−717.074 02	0.0			MP2/II[b]
6b	C_2	−713.685 99	<0.1	114.0	1 (−15)	HF/I
		−715.435 51	−0.6	113.1	0	HF/II
		−714.781 03	<0.1			MP2/I
		−717.074 10	−<0.1			MP2/II[b]

[a] Geometry optimized at MP2/II. [b] Geometry optimized at MP2/I.

minimum at MP2/II. Calculations at the CCSD(T) level indicate also that the open form of $(CH_3)_2CuLi$ is lower in energy than the cyclic structure. The isomeric form **3d** is 2.2 kcal/mol more stable than **3a** (CCSD(T)/III, Table 3).[36] This is an important result, because previous theoretical studies of the addition of **3** to olefins considered only the cyclic form.[13]

The calculated reaction energy D_o for the formation of the global energy minimum form **3d** from $CuCH_3$ and $LiCH_3$ is 49.5, 35.5, and 63.3 kcal/mol at MP2/II, MP3/II, and MP4/II, respectively. At MP2/III D_o is 50.2 kcal/mol (Table 4, reaction III). As for reaction I and II (Table 4) the oscillation of the D_o values can be explained by the change of the coordination number of copper in these reactions. The D_o values at MP2/II (49.5

---

[36] (a) A lower energy (−5.3 kcal/mol) for the open form **3d** than for the cyclic structure **3a** has also been calculated at the MP2 level using an all-electron basis set for Cu [8s6[4d1f][36b–d] and 6-31G+G(d) basis set for the other atoms. Böhme, M.; Frenking, G. Unpublished. (b) Wachters, A. J. H. *J. Chem. Phys.* **1970**, *52*, 1033. (c) Hay, P. J. *Ibid.* **1977**, *66*, 4377. (d) Stewart, R. F. *Ibid.* **1970**, *52*, 431.

Table 4. Calculated Reaction Energies ΔE Using Geometries Optimized at MP2/II for the Reactions I–IV[a]

$$CH_3^{\bullet} + Cu \rightarrow CH_3Cu\ (\mathbf{1}) \qquad (I)$$

$$CuCH_3\ (\mathbf{1}) + CH_3^- \rightarrow (CH_3)_2Cu^-\ (\mathbf{2a}) \qquad (II)$$

$$CuCH_3\ (\mathbf{1}) + LiCH_3 \rightarrow (CH_3)_2CuLi\ (\mathbf{3d}) \qquad (III)$$

$$(CH_3)_2CuLi\ (\mathbf{3d}) + H_2O \rightarrow (CH_3)_2CuLi{\cdot}H_2O\ (\mathbf{4d}) \qquad (IV)$$

$$2(CH_3)_2CuLi\ (\mathbf{3d}) \rightarrow ((CH_3)_2CuLi)_2\ (\mathbf{5}) \qquad (V)$$

	reacn				
method	I	II	III	IV	V
MP2/II	50.0 (47.0)	108.9 (106.1)	50.8 (49.5)	30.4 (28.2)	71.2 (68.8)
MP3/II	39.5 (36.5)	96.2 (93.4)	36.8 (35.5)	31.8 (29.6)	73.4 (71.0)
MP4/II	56.3 (53.3)	118.6 (115.8)	64.6 (63.3)	27.6 (25.4)	71.9 (69.5)
MP2/III	51.7 (48.7)	86.3 (83.5)	51.5 (50.2)	25.3 (23.1)	
CCSD(T)/III	48.0 (45.0)	80.5 (77.5)	45.8 (42.8)		

[a] Values in parentheses include zero-point energy corrections calculated at MP2/II. All values are given in kcal/mol.

kcal/mol) and at MP2/III (50.2 kcal/mol) show that the basis set II is nearly saturated. The CCSD(T)/III value for the complex formation energy of **3d** is $D_0 = 42.8$ kcal/mol (Table 4).

We also studied the effect of solvent complexation upon the structures and relative energies of the bridged (**3a**,**b**) and open (**3c**,**d**) forms of **3**. Addition of one water molecule to Li in **3a**,**b** gives structures **4a**,**b** (Figure 1). The Cu–C bonds are shorter and the Li–C distances are longer in **4a**,**b** than in the uncomplexed molecules **3a**,**b**. Structure **4a** is a transition state at HF/I and HF/II (one imaginary frequency) and a higher order saddle point at MP2/II (two imaginary frequencies). Structure **4b** has even three imaginary modes at the HF/I level. Therefore, no further calculations were performed for **4b**. Geometry optimization, without symmetry constraints results in the open forms **4c**,**d**, which have a nearly linear C–Cu–C moiety and a monocoordinated Li. At HF/I and HF/II structure **4c** is an energy minimum, but optimization of **4c** at MP2/II gives structure **4d**, which is a minimum at this level of theory. The stabilization energy of **4d** due to complexation by one water molecule is −25.4 kcal/mol at MP4/II//MP2/II (Table 4, reaction IV). The energy difference between **4a** and **4d** is 5.4 kcal/mol at MP4/II//MP2/II in favor of **4d** (Table 3). The energy difference between the uncomplexed forms **3a** and **3d** at MP4/II//MP2/II is 6.2 kcal/mol in favor of **3d**. It follows that the complexation of **3** by one water molecule has little influence upon the relative energy of the bridged and open forms of **3** and **4**, respectively. Thus, theory predicts that the monomeric form of Gilman's reagent $(CH_3)CuLi$ has an open (noncyclic) structure in the gas phase as well as in solution.

Dimerization of **3d** leads to $[(CH_3)_2CuLi]_2$ (**5**). Experimental studies have shown that Gilman's reagent is a dimer in diethyl ether.[37,38] The results of ^{1}H-NMR and solution X-ray scattering measurement of **5** in ether indicate that **5** has a cyclic structure with approximate D_{2h} symmetry.[38] The X-ray structure analysis of the phenyl derivative of Gilman's reagent $[(C_6H_5)_2CuLi]_2$[39] reveals a twisted eight-membered ring with nearly linear R_2Cu fragments, which are linked by the Li counterions. The Li atoms are tricoordinated; the additional coordination site is occupied by an ether molecule.[39]

We calculated $[(CH_3)_2CuLi]_2$ (**5**) with a planar ring structure with D_{2h} symmetry (Figure 1). Structure **5** is a minimum at all three levels of theory. The Cu–C bond distances are 2.057 Å at HF/I, 2.066 Å at HF/II, and 1.968 Å at MP2/II. The $(CH_3)_2Cu$ fragments are nearly linear (α(C–Cu–C) = 172–174°). Also, the C–Li–C angles are only slightly bent (α(C–Li–C) = 160–167°). The calculated Cu–Cu distances are 3.878, 3.904, and 3.826 Å at HF/I, HF/II, and MP2/II, respectively. A Cu–Cu distance of 4.4 ± 0.7 Å was estimated from the X-ray scattering pattern of **5** in ether solution.[38] X-ray studies of *solid* cuprates containing larger organic groups give Cu–Cu distances between 2.7 and 3.0 Å.[4] The calculated dimerization energy of **3d** yielding **5** (reaction V, Table 4) is 69.5 kcal/mol at MP4/II//MP2/II. We optimized **5** using different starting geometries such as a twisted form of **5**, dimeric forms of **3a**, and a structure with a tetrahedral Cu_2Li_2 core. The only energy minimum form which could be found is the D_{2h} form **5**.

Geometry optimization of **5** complexed by one water molecule at each Li atom gives a slightly twisted ring structure for the isomeric forms **6a**,**b** (Figure 1). The optimized geometries of $[(CH_3)_2CuLi]_2{\cdot}2H_2O$ (**6a**,**b**) gave C_{2v} and C_2 symmetry, respectively. The complexation of the lithium atoms yields significantly longer Li–C distances compared to **5** (Table 1). The Cu–C bond lengths are predicted at the MP2 level to be slightly longer in **6a**,**b** than in **5**. The energy difference between the isomeric forms **6a**,**b** is very small at all levels of theory (Table 3). The two structures differ only slightly in the torsion angle $\tau(C^2\text{–}Cu\text{–}C^4\text{–}Li)$ (Table 1), which is a measure of the degree of twisting.

A comparison with the crystal structure of $[Li(OEt)_2)CuPh_2]_2$[39] (**7**) shows that **6** has a less twisted ring than **7**, probably due to the different steric interactions in the two compounds. This explains why the internuclear Cu–Cu distance in **6a** (HF/I, 3.753 Å; HF/II, 3.758 Å; MP2/I, 3.763 Å) and in **6b** (HF/I, 3.731 Å, HF/II, 3.588 Å; MP2/I, 3.775 Å) are longer than in **7** (2.87 Å). Except for the Cu–Cu distance, the calculated geometries for **6a**,**b** are very similar to that for the experimentally obtained structure **7**. As noted above, experimental studies of **5** in ether showed that the complex has nearly D_{2h} symmetry. This is in excellent agreement with the optimized structures of **6a**,**b** at the MP2/I level, which deviate only slightly from D_{2h} symmetry (twisting angle τ = 177.0° (**6a**), 177.5° (**6b**)).

In further studies we investigated the electron density distribution of **1**, **2a**, **3a**,**d**, **4a**,**d**, **5**, and **6b** using the topological analysis of the electron density distribution developed by Bader and co-workers.[10] Figure 2 summarizes the Laplacian distribution for **1**, **2a**, **3a**,**d**, **4a**,**d**, **5**, and **6b**. Table 5 gives the results of the topological analysis of the wave function.

The contour line diagram of **1** (Figure 2a) reflects a nearly isotropical Laplacian distribution with an area of charge depletion ($\nabla^2\varrho(\mathbf{r}) > 0$, dashed lines) around Cu. The carbon atom has an area of charge concentration ($\nabla^2\varrho(\mathbf{r}) < 0$, solid lines) pointing toward the copper atom. The shape of the Laplacian distribution suggests that the Cu–C bonding in **1** is best described as an interaction between a methyl anion and copper cation.

---

(37) Lipshutz, B. H.; Kozlowski, J. A.; Breneman, C. M. *J. Am. Chem. Soc.* **1985**, *107*, 3197.

(38) Pearson, R. G.; Gregory, C. D. *J. Am. Chem. Soc.* **1976**, *98*, 4098.

(39) Lorenzen, N. P.; Weiss, E. *Angew. Chem.* **1990**, *102*, 322; *Angew. Chem., Int. Ed. Engl.* **1990**, *102*, 300.

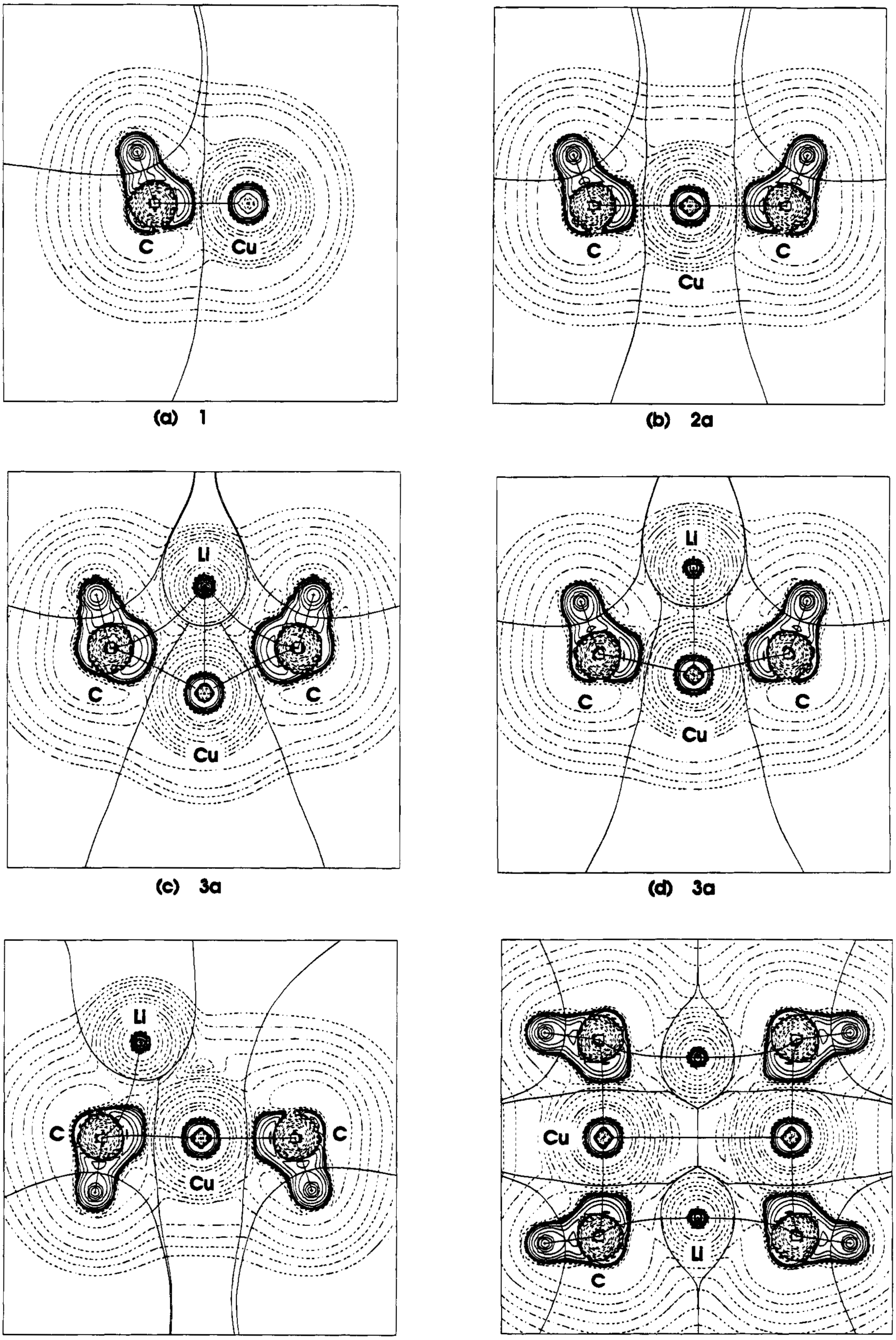

(a) 1

(b) 2a

(c) 3a

(d) 3a

(e) 3d

(f) 5

Figure 2. Contour line diagrams of the Laplacian distribution $\nabla^2\varrho(\mathbf{r})$: (a) Structure **1** at MP2/II; (b) structure **2a** at MP2/II; (c) structure **3a** at HF/II; (d) structure **3a** at MP2/II; (e) structure **3d** at MP2/II; (f) structure **5** at MP2/II. Dashed lines indicate charge depletion ($\nabla^2\varrho(\mathbf{r}) > 0$); solid lines indicate charge concentration ($\nabla^2\varrho(\mathbf{r}) < 0$). The solid lines connecting the atomic nuclei are the bond paths; the solid lines separating the atomic nuclei indicate the zero-flux surfaces in the molecular plane. The crossing points of the bond paths and zero-flux surfaces are the bond critical points $\mathbf{r}_b$.

Table 5. Results of the Topological Analysis of the Wave Function for 1, 2a, 3a,d, 4a,d, 5, and 6b: Laplacian Concentration $-\nabla^2\varrho(\mathbf{r}_b)$ (e Å^{-5}), Energy Density (hartree Å^{-3}), and Electron Density $\varrho(\mathbf{r}_b)$ (e Å^{-3}) at the Bond Critical Point $\mathbf{r}_b$ (R Related to R(X–Y) = 1)

no.	method	X–Y	$\varrho(\mathbf{r}_b)$	$-\nabla^2\varrho(\mathbf{r}_b)$	H_b	$R(X-\mathbf{r}_b)$	$R(\mathbf{r}_b-Y)$
1	MP2/II	Cu–C	0.748	6.639	−0.252	0.506	0.494
2a	MP2/II	Cu–C^1	0.710	8.033	−0.218	0.486	0.514
3a	HF/II	Cu–Li	0.143	2.411	0.004	0.633	0.367
		Cu–C	0.481	6.596	−0.062	0.477	0.523
		Li–C	0.149	2.578	0.023	0.343	0.657
3a	MP2/II	Cu–Li	0.182	2.689	−0.011	0.638	0.362
		Cu–C	0.692	7.945	−0.204	0.490	0.510
3d	MP2/II	Li–C^1	0.205	4.006	0.032	0.356	0.644
		Cu–C^1	0.636	7.782	−0.169	0.482	0.518
		Cu–C^2	0.787	7.580	−0.280	0.496	0.504
4a	MP2/II	Cu–Li	0.175	2.488	−0.012	0.639	0.361
		Cu–C	0.712	8.002	−0.220	0.491	0.509
4d	MP2/II	Li–C^1	0.184	3.664	0.033	0.360	0.640
		Cu–C^1	0.654	7.900	−0.180	0.484	0.516
		Cu–C^2	0.738	7.841	−0.241	0.493	0.507
5	MP2/II	Cu–Cu	0.061	0.279	−0.002	0.500	0.500
		Li–Li	0.061	0.279	−0.002	0.500	0.500
		Cu–C	0.695	7.892	−0.208	0.489	0.511
		Li–C	0.186	3.879	0.035	0.366	0.634
6b	MP2/II^a	Cu–C	0.670	7.602	−0.199	0.488	0.512
		Li–C	0.129	2.279	0.024	0.352	0.648

^{a} Geometry optimized at MP2/I.

The NBO analysis reveals a partial negative charge of −0.54 e at CH_3 and a positive charge of +0.54 at Cu (Table 6). The energy density at the bond critical point of the Cu–C bond of **1** (H_b = −0.252, Table 5) indicates largely ionic character but that there are clearly covalent contributions. A negative value of H_b has been suggested to indicate covalent bonding with typical values for C–C and C–H bonds between −1 and −3, while ionic and van der Waals interactions are characterized by $H_b \geq 0$.[40] The location of the bond critical point $\mathbf{r}_b$ is nearly in the middle of the Cu–C bond ($R(\text{Cu}-\mathbf{r}_b)$ = 0.506).

The Laplacian distribution for **2a** shows (Figure 2b) a similar shape for the Cu–C bonds as in **1**. The results of the topological analysis indicate slightly less covalent contributions to the Cu–C bonds in **2a** than in **1** (H_b = −0.218). The additional negative charge is concentrated at the methyl groups. The partial charge at Cu in **2a** calculated by the NBO partitioning scheme is +0.48 (Table 6), which is nearly the same as in **1**.

The contour line diagram of **3a** (Figure 2c, HF/II//HF/II; Figure 2d, MP2/II/MP2/II) indicates a nearly isotropical Laplacian distribution with an area of charge depletion around Li and Cu. It is illustrative to discuss the electronic structure of **3a** at the HF/II and MP2/II level of theory, because the two theoretical levels lead to qualitatively different interpretations of the electronic structure. From the analysis of the electron density distribution of the HF/II level, result bond paths between Cu–C, Cu–Li, Li–C, and two ring critical points for **3a**. Thus, the topology of the electronic structure at HF/II indicates that **3a** should be considered as a bicyclic compound. The dropletlike appendix of charge concentration at the carbon atoms points toward the center of the bicyclic ring. The H_b values for the Cu–C and Li–C bonds are nearly zero, indicating purely ionic bonds. The MP2/II results are different. At the correlated level the bond paths between Li and the carbon atoms disappear (Figure 2d). The area of charge concentration at C is clearly directed toward Cu. The energy densities at the bond critical points for the Cu–C bonds show distinct covalent contributions (H_b = −0.204). It is noteworthy that the calculated partial charges at the methyl groups in the neutral compound **3a** have the same negative values (−0.74, Table 6) as in the anion **2a**. Thus, the bonding situation in **3a** analyzed at the MP2/II level is characterized by polar Cu–C bonds similar to **2** with an ionic bonded Li atom bridging the carbon atoms. This result is in agreement with an earlier MO study by Stewart et al.[17] They found that the methyl groups in $[(CH_3)_2CuLi]_2$ have lone pair electrons which are almost exclusively bonded to copper rather than to lithium.

The Laplacian distribution of **3d** is very similar to **3a**, but the bond paths and critical points indicate a slightly different type of electronic structure. Unlike **3a**, the isomeric form **3d** has a bond path between Li and C^1. The topology of the electronic structure indicates that **3d** has an open noncyclic form with the Li atom bonded only to C. The Li–C bond is purely ionic as revealed by the H_b value 0.032 (Table 5). The Laplacian distribution pictured in Figure 2e explains the acute Cu–C^1–Li angle in **3d**. The electronic charge at the negatively charged carbon atom exhibits an area of charge concentration toward the Cu atom. The positively charged Li atom is attracted by the accumulation of charge at C^1 in the Cu–C bonding region, which is only slightly distorted by the Li cation. This has nothing to do with Cu–Li attractive interactions, which might be expected because of the short Cu–Li distance. The H_b values for the Cu–C bonds of **3d** indicate covalent contributions (−0.169, −0.280).

The Laplacian distribution of the water-complexed structures **4a,d** shows very little differences relative to the uncomplexed forms **3a,d**, respectively. Therefore, they are not reproduced here. Table 5 shows that the results of the topological analysis are very similar for the respective monomeric lithium cuprates with and without water.

The Laplacian distribution for the dimeric cuprate **5** (Figure 2f) at the MP2/II level gives bond paths between C and Li, unlike the monomeric form **3a**, which has only Cu–C bond paths (Figure 2d). The shape of the Laplacian distribution demonstrates that the methyl groups in **5** resemble the CH_3 group of **3d** (Figure 2e). The Cu–C bonds in **5** are partially covalent (H_b = −0.208). The Laplacian distributions of **6a,b** are very similar to **5**. Therefore, they are not shown here. The analysis of the electron density distribution at MP2/II using the MP2/I optimized geometry indicates that the complexation of Li by one water molecule in **6** has little influence upon the nature of the copper bonding, similar to the situation in the case of **4**.

We also studied the electronic structure of **1**, **2a**, **3a,d**, **5**, and **6b** using the natural bond orbital analysis.[11] (Table 6). The results (Table 6) reveal a nearly complete occupation of the 3d(Cu) orbitals (occupation > 9.8 e), while the 4p(Cu) orbitals remain practically unoccupied. Except for the 4s(Cu) orbital, the calculated metal AO populations do not differ significantly from the formal population ($4s^0 3d^{10} 4p^0$) of Cu$^+$. The population of the 4s orbital at Cu is between 0.52 e (**1** and **6b**) and 0.68 e (**2a**). The partial charge at Cu is between +0.48 (**2a**) and +0.59 (**6b**).

The methyl groups in **1**–**6b** always carry a significant negative partial charge. The NOB analysis indicates that the Cu–C bonds can be interpreted as the result of charge donation from the lone pair electrons from the

Table 6. Results of the NBO Analysis Calculated at HF/II Using Geometries at MP2/II

		population (Cu)			Cu—C Bond[a]					charges[b]	
no.	sym	4s	3d	4p	pop.	% Cu	% 4s	% 4p	% 3d	q_{Cu}	q_{CH_3}
1	C_{3v}	0.52	9.93	0.01	2.0	23.23	95.06	1.12	3.73	0.54	−0.54
2a	D_{3h}	0.68	9.83	0.01	2.0	15.42	88.93	0.98	10.09	0.48	−0.74
3a	C_{2v}	0.54	9.88	0.01	1.96	13.45	91.89	1.94	6.17	0.57	−0.74
3d	C_1	0.65	9.83	0.01	1.97	18.85	89.87	1.06	9.07	0.50	−0.77 −0.65
4a	C_{2v}	0.57	9.86	0.01	2.0	14.03	91.62	1.42	6.96	0.55	−0.73
4d	C_1	0.59	9.86	0.01	1.97	15.66	91.21	1.05	7.74	0.54	−0.76 −0.70
5	D_{2h}	0.58	9.85	0.01	1.95	13.90	91.30	0.69	8.02	0.57	−0.71
6b[c]	C_2	0.57	9.85	0.01	1.94	13.86	91.38	0.67	7.95	0.57	−0.71

[a] % Cu gives the contribution of the Cu—C bond orbital at Cu; % 4s, % 4p, and % 3d give the hybridization of the Cu—C bond at Cu. [b] q_{Cu} and q_{CH_3} are the partial charges at Cu and CH_3, respectively. [c] Geometry optimized at MP2/I.

methyl anion into the formally empty Cu 4s orbital. Back-donation of the 3d electrons from Cu into π^* orbitals of the methyl group is negligible; the Cu—C bond has mainly s character (~90%). The rather small contribution of Cu orbitals to the Cu—C bonds (12−23%) demonstrates the distinct polarization toward the carbon atom. This is in agreement with the shape of the Laplacian distribution shown in Figure 2.

The breakdown of the electronic structures of **2**−**6b** into bond orbitals gives only one Cu—C bond orbital in the CH_3—Cu—CH_3 fragments. The orbital of the second bond is characterized as a carbon lone pair MO. This result can be explained in terms of Lewis structures, e.g. of the anion **2**:

$$CH_3\text{—}Cu\ CH_3^- \leftrightarrow CH_3^-\ Cu\text{—}CH_3$$

A final question concerns the nature of the lithium bonding in structures **3**−**6**. The topological analysis and the NBO partitioning scheme indicate that the lithium bonding is practically only ionic. There are no C—Li or Cu—Li bonds found in the NBO scheme, and the topological analysis shows that the energy density at the bond critical points of the Li bonds is always positive, which is a strong indication for an ionic bond.[40] In particular, there are no two-electron three-center bonds in the dimer **5**, which should rather be considered as a complex held together by the Coulombic interactions between the positively charged Li and negatively charged methyl groups.

Summary

The optimized geometries of the copper compounds **1**−**6** at the MP2 level of theory have Cu—C bond lengths which are in good agreement with the existing experimental data. At the HF level the Cu—C bond distances are too long. $CuCH_3$ (**1**) is predicted to have a Cu—C bond length of 1.923 Å. The Cu—C bond strength of **1** is calculated at the CCSD(T) level as D_0 = 45.0 kcal/mol. The dimethylcuprate anion **2** (D_{3h}) is predicted to have a slightly longer Cu—C bond (1.963 Å) than **1**. The formation of **2** from **1** + CH_3^- is calculated to be 77.5 kcal/mol exothermic. Geometry optimization of lithium dimethylcuprate (**3**), which is the monomeric form of Gilman's reagent, yields the open form **3d** with a nearly linear C—Cu—C arrangement and monocoordinated lithium as the global energy minimum structure. The cyclic form **3a** with lithium bridging the methyl groups is 2.2 kcal/mol higher in energy at the CCSD(T) level. The Cu—C bond lengths of **3d** are 1.916 and 2.009 Å, respectively. Complexation of the Li atom by one water molecule in the corresponding complex **4** has little influence upon the structural features. The open form **4d** is clearly more stable than the cyclic structure **4a**.

The dimeric form of Gilman's reagent **5** is predicted to have a cyclic planar geometry with D_{2h} symmetry. The optimized structure **5** exhibits nearly linear C—Cu—C and C—Li—C angles. The Cu—C bonds are calculated with a similar bond length (1.968 Å) as in the bridged isomer of the monomer form **3a** (1.971 Å). Complexation of **5** at the lithium atoms by two water molecules gives two energetically nearly degenerate forms **6a,b**, which have a slightly twisted cyclic structure. The Cu—C bond lengths in **6a,b** are a little longer (1.982 and 1.983 Å) than in **5**. The optimized geometries of **6a,b** are in good agreement with experimental studies of Gilman's reagent in ether solution.

The topological analysis of the electron density distribution of **1**−**6** shows that the Cu—C bonds are strongly polarized according to Cu^+—C^-. The energy density at the bond critical points indicates significant covalent contributions to the polar Cu—C bonds, while the Li—C bonds are purely ionic. The NBO analysis also indicates that the Cu—C bonds are clearly polarized toward the carbon atom; the contribution from Cu is only 13−24%. The copper bonding has mainly s character (88−95%). The partial charge at Cu is always ~+0.5 e.

In summary, the present calculations represent the most complete study of several forms of cuprates, providing valuable insight into the bonding. Further studies which address the question of the existence and possible electronic structure of higher order cuprates are in progress.

Acknowledgment. We thank Dr. James P. Snyder for stimulating discussions. This work was supported by the Deutsche Forschungsgemeinschaft and the Fonds der Chemischen Industrie. Excellent service by the Hochschulrechenzentrum of the Philipps-Universität Marburg is gratefully acknowledged. Additional computer time was provided by the HHLRZ Darmstadt and the HLRZ Jülich.

OM940139G

---

(40) Cremer, D.; Kraka, E. *Angew. Chem.* **1984**, *96*, 612; *Angew. Chem., Int. Ed. Engl.* **1984**, *96*, 627.